

SIMULATED AND EXPERIMENTAL INVESTIGATION OF THE NAP-OF-THE-EARTH MANOEUVRES FOR A HELICOPTER

Grzegorz Kowaleczko

Military University of Technology

ul. Kaliskiego 2, 00-908 Warsaw, Poland

e-mail: kowaleczko@wul.wat.waw.pl

Abstract

Results of a numerical simulation for selected spatial nap-of-the-earth manoeuvres of a helicopter are presented. A method of inverse dynamics has been used for this simulation. Results of simulation are compared with courses of parameters recorded during flights.

Introduction

The identification of helicopter flight characteristics is one of the most significant problems in the domain of flight dynamics. Knowledge of them is very important from the constructional (design phase) and operational points of view. However, the flight characteristics (or so called flight properties) of a helicopter are rarely well known even for aircraft, which have been used for years. This is mostly due to limitations put on by flight regulations. The second reason is the lack of objective criteria for estimation of the flight characteristics of a helicopter. The very first attempt of developing such criteria is the ADS norm (*Aeronautical Design Standard – Handling Qualities Requirements for Military Rotorcraft*) introduced not so far ago [1], [2].

The flight characteristics are especially important for the nap-of-the-earth flight studies. NoE flights are basic type of flights in secret missions - for instance military or anti-terrorist - in which a stealthy approach to the mission target, with utilisation of a natural cover, plays a decisive role. According to a different kind of studies from the three factors: manoeuvrability, electronic

interference warfare usage and armouring, the most important for a helicopter survival in a battlefield is the first mentioned. NoE flights almost often are performed on a helicopter manoeuvrability limits.

Because of that the knowledge of helicopter flight characteristics is extremely important, especially for newly designed aircraft - the lack of precise and reliable data in that domain may result in overestimation or underestimation of the aircraft performance and, consecutively, in an increased risk of tough missions.

Investigations of flight characteristics can be performed by two means. The first is based on data collected during test flights. In test flights there are performed maneuvers of many kinds. The dynamics of these maneuvers is gradually increased up to a helicopter performance limits. In such flights it is difficult to keep the safety limits. Many of helicopter constructional elements are exposed to extreme stresses. The method itself is expensive and hazardous. It demands a lot of experience from test pilots. The danger is connected with unexpected and non-typical reaction of the aircraft to control - a snatch up or a reversal-roll can occur.

Numerical simulation is the alternative method to identify helicopter flight characteristics. It consists in theoretical modelling of helicopter flight during a stated manoeuvre. Results of such investigations have a limited credibility only. They would be better if the applied mathematical model of a helicopter better reflects real physical phenomena occurred during flight.

Practice shows that the best results of flight properties investigations can be obtained by simultaneous usage of both methods. Such approach allows to improve the mathematical

model of a helicopter when results of numerical simulation are compared with data from the flight recorder.

At the same time it is possible to anticipate theoretically behaviour of a helicopter at not precisely specified flight conditions. It makes easier to plan and perform test flights, shows potential hazards and gives indications about necessary control. Beyond any doubts, simultaneous usage of both methods gives the best results and is optimal.

1. Formulation of the problem

A nonlinear model of a helicopter is applied for calculations where the fuselage of a helicopter is treated as a rigid body. This model allows to determine linear and angular displacements of the fuselage. Dynamics of movable parts of the helicopter is not included into consideration. In this case only spatial motion of rigid fuselage forced by aerodynamic forces is considered. These forces are produced by the main and the tail rotors. The main rotor is considered separately. It is treated as a cone. Only global parameters of this cone are determined. These parameters show position of this cone in the fixed coordinate system. At the same time the average values of forces and moments are calculated. All nonlinear inertial cross-couplings are included into consideration. The only simplifications are connected with modelling of blades aerodynamics. They are determined by the used method of calculation of forces produced by blades.

This mathematical model of the helicopter is described in detail in [4].

1.1. Dynamics of the fuselage

Assuming, spatial motion of the helicopter is described by:

- equations of translatory motion of the helicopter;
- equations of equilibrium of moments about the centre of mass of the fuselage;
- kinematic relations enabling to determine spatial configuration of the helicopter and its trajectory.

Finally the set of twelve nonlinear differential equations is obtained. It can be presented in the following form:

$$\frac{d\bar{X}^*}{dt} = \bar{X}^* = \bar{G}^*(t, \bar{X}, \bar{S}) \quad (1.1)$$

where: $\bar{X}^* = (U, V, W, P, Q, R, \Theta, \Phi, \Psi, x_g, y_g, z_g)^T$ is the vector of the helicopter motion parameters. We have:

- linear velocities U, V, W and angular velocities of the fuselage P, Q, R ;
- angles and coordinates describing spatial orientation and position of the fuselage $\Theta, \Phi, \Psi, x_g, y_g, z_g$;

$\bar{S} = (\theta_0, \kappa_s, \eta_s, \varphi_{tr})^T$ is the vector of control parameters:

- θ_0 - is the angle of collective pitch of the main rotor;
- κ_s - is the control angle in the longitudinal motion;
- η_s - is the control angle in the lateral motion;
- φ_{tr} - is the angle of collective pitch of the tail rotor.

1.2. Dynamics of the angular motion of the main rotor and the model of regulation of rotation

Dynamics of the angular motion of the main rotor is also considered. The phenomena of deceleration and acceleration of engines is included into account.

For the purpose of taking into account the dynamics of angular motion of the main rotor the following equation is added:

$$I_{mr} \dot{\omega} = N_d + N_{ps} \quad (1.2)$$

where:

- I_{mr} - the inertia moment of the main rotor;
- N_d - the drag moment of aerodynamics forces;
- N_{ps} - the moment of power system.

It is assumed that the angular velocity at the time t_k is equal to the nominal angular velocity ω_0 . If at the next moment $t_{k+1} = t_k + \Delta t$ this velocity is different and equal to $\omega(t_{k+1}) = \omega_0 + \Delta\omega$ and than the reaction of the power transmission system is induced. The change of the moment N_{ps} is equal to:

$$\Delta N_{ps} = \frac{\partial N_{ps}}{\partial \omega} \Delta \omega \quad (1.3)$$

The derivative $\frac{\partial N_{ps}}{\partial \omega}$ may be transformed

as follows:

$$\frac{\partial N_{ps}}{\partial \omega} = \frac{\partial N_{ps}}{\partial t} \frac{\partial t}{\partial \omega} = \frac{\partial N_{ps}}{\partial t} \frac{\Delta t}{\Delta \omega} = \frac{\partial N_{ps}}{\partial t} \frac{t_{k+1} - t_k}{\omega(t_{k+1}) - \omega_0} \quad (1.4)$$

Two different values of the derivative $\frac{\partial N_{ps}}{\partial t}$ are used - for the acceleration and deceleration cases. They have been obtained experimentally.

In spite of its simplicity the model is sufficient for the analysis of many different manoeuvres.

Finally, a set of thirteen differential equations is obtained:

$$\frac{d\bar{X}}{dt} = \bar{X} = \bar{G}(t, \bar{X}, \bar{S}) \quad (1.5)$$

where $\bar{X} = (U, V, W, P, Q, R, \Theta, \Phi, \Psi, x_g, y_g, z_g, \omega)^T$ is the final vector of helicopter motion parameters.

1.3. Dynamics of the main rotor

Motions of blades are considered separately, simultaneously with motions of a fuselage - average values of forces and moments produced by the main rotor and acting on the fuselage are calculated. The position of the main rotor cone is determined by resolving a set of nonlinear algebraic equations:

$$\hat{L}(\bar{X}, \bar{S}, \bar{\beta}) \bar{\beta} = \bar{F}(\bar{X}, \bar{S}, \bar{\beta}) \quad (1.6)$$

where $\bar{\beta} = (a_0, a_1, b_1)$ is a vector determining orientation of the cone in relation to a fuselage.

2. Inverse simulation algorithm

In this paper, a specific numerical method of a solution of the inverse problem is applied. It is based on linearization of the considered problem around a current position of the object in the state space. This method was successfully applied with success to dynamic flight problems of aeroplanes and helicopters [5]-[9]. Its description is presented below.

The set (1.5) can be integrated using one of the numerical methods (for instance the Runge-Kutta method).

The output vector $\bar{Y} \in \mathfrak{R}^n$ is uniquely determined by the vector of flight parameters \bar{X} .

$$\bar{Y} = \bar{D}(\bar{X}) \quad (2.1)$$

In the present considerations both vectors are the same:

$$\bar{Y} = \bar{X} \quad (2.2)$$

The set (1.5) is completed by the following initial conditions:

$$\bar{X}(t_0) = \bar{X}_0 \quad (2.3)$$

In the considered case, the fundamental problem is to determine the control vector $\bar{S}(t)$ for the defined output vector $\bar{Y}_z(t)$, which describes constraints of the object motion.

Problem is made discrete for successive time points $t_0, \dots, t_k, t_{k+1}, \dots, t_N$. For each instant t_{k+1} , the vector $\bar{Y}_z(t_{k+1})$ is defined by constraints of motion. The vector $\bar{X}(t_{k+1})$ is also calculated as a result of integration of the set (1.5) in the time interval from t_k to t_{k+1} . This interval is determined in the way which preserves the stability of final solution. Because the described procedure requires the one constant time step and because of a nonlinearity of the problem, this step is determined by numerical experiments. This means that several simulations should be performed with decreasing time intervals up to the moment when two convergent solutions are obtained. The method is in agreement with the Runge-Kutta method with different time interval. The time interval is dependent upon every individual problem. According to (1.5), because the derivative $\frac{d\bar{X}}{dt}$ depends on the control vector $\bar{S}(t_k)$, the calculated value $\bar{X}(t_{k+1})$ also depends on this control vector. The vector $\bar{Y}(t_{k+1})$ determined on the basis of relation (1.7) has to be equal to specified value $\bar{Y}_z(t_{k+1})$. Difference between the calculated value of the vector $\bar{Y}(t_{k+1})$ and the constrained vector $\bar{Y}_z(t_{k+1})$ is the basis for the calculation of a corrected value of control vector $\bar{S}(t_k)$.

This procedure has an iterative character. It means that for each time point t_k , a finite number of iterations are performed till the assumed compatibility between vectors \bar{Y} and \bar{Y}_z is obtained. In the i -th step of iteration the following operations are performed:

1. On the basis of a known $\bar{X}(t_k)$ and $\bar{S}^{(m)}(t_k)$ making use of (1.5), the derivative is calculated:

$$\bar{X}^{(m)}(t_k) = \bar{G}[t_k, \bar{X}(t_k), \bar{S}^{(m)}(t_k)] \quad (2.4)$$

2. The value of flight parameters and output vector at the time point t_{k+1} is determined by numerical integration of relation (2.4):

$$\bar{X}^{(m)}(t_{k+1}) = \bar{X}(t_k) + \int_{t_k}^{t_{k+1}} \bar{X}^{(m)}(t_k) dt \quad (2.5)$$

$$\bar{Y}^{(m)}(t_{k+1}) = \bar{D}[\bar{X}^{(m)}(t_{k+1})] \quad (2.6)$$

3. The difference between defined output vector $\bar{Y}_z(t_{k+1})$ and the vector calculated from (2.6) is determined:

$$\Delta \bar{Y}^{(m)}(t_{k+1}) = \bar{Y}_z(t_{k+1}) - \bar{Y}^{(m)}(t_{k+1}) \quad (2.7)$$

If this difference is smaller than the specified accuracy $\mathcal{E}_{\bar{Y}}$, calculations are continued at next time point t_{k+2} taking as initial data the vector of flight parameters and the control vector determined at time t_{k+1} . If this difference $\Delta \bar{Y}^{(m)}(t_{k+1})$ is greater than $\mathcal{E}_{\bar{Y}}$ the improved value of control vector $\bar{S}^{(m+1)}(t_k)$ is calculated. For this purpose Newton method is applied. According to this method an expression for $\bar{S}^{(m+1)}(t_k)$ is as follows:

$$\bar{S}^{(m+1)}(t_k) = \bar{S}^{(m)}(t_k) + \mathbf{J}^{-1} \Delta \bar{Y}^{(m)}(t_{k+1}) \quad (2.8)$$

where \mathbf{J} is the Jakobian. Its elements are determined by formula:

$$J_{ij}(t_k) = \frac{\partial[\Delta \bar{Y}_i^{(m)}(t_{k+1})]}{\partial \bar{S}_j^{(m)}(t_k)} = \frac{\partial \bar{Y}_i^{(m)}(t_{k+1})}{\partial \bar{S}_j^{(m)}(t_k)} \quad (2.9)$$

Because the considered problem is solved numerically, then the following differential scheme is applied:

$$J_{ij}(t_k) = \frac{Y_i^{(m)}[t_{k+1}, S_j^{(m)}(t_k) + \delta S_j^{(m)}] - Y_i^{(m)}[t_{k+1}, S_j^{(m)}(t_k) - \delta S_j^{(m)}]}{2\delta S_j^{(m)}}$$

The expression (2.8) is a result of the following procedure:

The output vector $\bar{Y}^{(m)}(t_{k+1})$ is calculated at the time point t_{k+1} at m -th iteration. It depends on the flight parameters vectors $\bar{X}(t_k)$ and the control vector $\bar{S}^{(m)}(t_k)$, which are determined at the previous time point t_k .

If the calculations are performed again for a modified value of the control vector:

$$\bar{S}^{(m+1)}(t_k) = \bar{S}^{(m)}(t_k) + \Delta \bar{S}^{(m)}(t_k), \quad (2.10)$$

one can obtain a new value of the output vector $\bar{Y}^{(m+1)}(t_{k+1})$ for the $(m+1)$ -th iteration. Making use of the Taylor series and taking into account only linear part of the expansion in series, one can assume that:

$$\bar{Y}^{(m+1)}(t_{k+1}) = \bar{Y}^{(m)}(t_{k+1}) + \mathbf{J} \Delta \bar{S}^{(m)}(t_k) \quad (2.11)$$

where Jacobian elements are determined by the relation (2.9). Using relation (2.11), after elementary transformations, one can obtain formula (2.8), which allows to calculate the control vector at time t_k for the $(m+1)$ -th iteration $\bar{S}^{(m+1)}(t_k)$. It is assumed that the calculated value of the output vector $\bar{Y}^{(m+1)}(t_{k+1})$ has to be equal to the determined value $\bar{Y}^{(m+1)}(t_{k+1}) = \bar{Y}_z(t_{k+1})$. It is taken into account in the relation (2.7).

3. Simulation of selected helicopter spatial manoeuvres

Many numerical simulations for different nap-of-the-earth manoeuvres were performed. They were: bob up and bob down, bob up to hover, acceleration and deceleration, slalom, sidestep and turn in hover. Results of some of them for a Polish helicopter *Sokol* are shown below. The presented above method of inverse dynamics analysis was used for this simulation. The time courses of selected recorded flight parameters were taken as the constraints. Selection of these parameters was performed in order to the complete description of certain aircraft manoeuvres. But for all cases, the following role was obligated: among four selected parameters, which were the constraints, two were the longitudinal parameters (two from U, W, Q, Θ), and two other were connected with lateral motion (two from V, P, R, Φ, Ψ).

3.1. The bob up and bob down manoeuvre

This manoeuvre is characterised by the rapid changes of the hover altitude. At the beginning this altitude increases. Next it is stabilized for at least two seconds. Finally the altitude decreases. The manoeuvre like this is particularly important for the military missions – it corresponds to the attack with fixed guns. As it was shown in [1] attacks performed during the

horizontal flight or during the hover are the most effective methods of attack for military helicopters. For this reason the ability of the helicopter to perform a rapid jump from behind an utilised protection and than hide again is very important. The time when the helicopter is over the protection should be minimised. It is limited by the time necessary to detect and to recognise a target and time of aiming.

It was assumed that the considered bob up and bob down manoeuvre was performed on the vertical plane without rolling and yawing. According to these conditions the angular velocities P and R were equal to zero:

$$P(t), R(t) = 0 \quad (3.1)$$

Additionally one assumed that the pitch angle Θ is constant. Under this condition it is easier to localise the target and to destroy it. This means that the pitching angular velocity is equal to zero:

$$Q(t) = 0 \quad (3.2)$$

The last constraint (connected with the longitudinal motion) describes changes of the vertical velocity (3.3):

$$W(t) = \begin{cases} 0 & \text{for } t < t_{m1W} \text{ or } t > t_{m3W} + T_{d3W} \\ \frac{W_1}{16} \left(\cos 3\pi \frac{t-t_{m1W}}{T_{d1W}} - 9 \cos \pi \frac{t-t_{m1W}}{T_{d1W}} + 8 \right) & \text{for } t_{m1W} \leq t < t_{m1W} + T_{d1W} \\ W_1 & \text{for } t_{m1W} + T_{d1W} \leq t < t_{m2W} \\ \frac{W_1 + W_2}{16} \left(\cos 3\pi \frac{t-t_{m2W}}{T_{d2W}} - 9 \cos \pi \frac{t-t_{m2W}}{T_{d2W}} + 8 \right) & \text{for } t_{m2W} \leq t < t_{m2W} + T_{d2W} \\ W_1 + W_2 & \text{for } t_{m2W} + T_{d2W} \leq t < t_{m3W} \\ \frac{W_1 + W_2 + W_3}{16} \left(\cos 3\pi \frac{t-t_{m3W}}{T_{d3W}} - 9 \cos \pi \frac{t-t_{m3W}}{T_{d3W}} + 8 \right) & \text{for } t_{m3W} \leq t \leq t_{m3W} + T_{d3W} \end{cases}$$

where t_m corresponds to the beginning of increase or decrease of the parameter. T_d is the period of the change and W_i are amplitudes of successive changes. The sum $W_1 + W_2 + W_3$ should be equal to zero. This guarantees that the manoeuvre is finished at the hover.

All these parameters were determined on the basis of data recorded during real flight. It was assumed that: $t_{m1W} = 0s$, $T_{d1W} = 2s$, $t_{m2W} = 2s$, $T_{d2W} = 4s$, $t_{m3W} = 6s$, $T_{d3W} = 2s$, $W_1 = -6m/s$, $W_2 = 12.5m/s$, $W_3 = -6.5m/s$.

Figures 2, 3, 5, 6, 8 show time courses of selected flight parameters obtained from the numerical simulation. They are compared with courses recorded during the test flight /fig.1, 4, 7/.

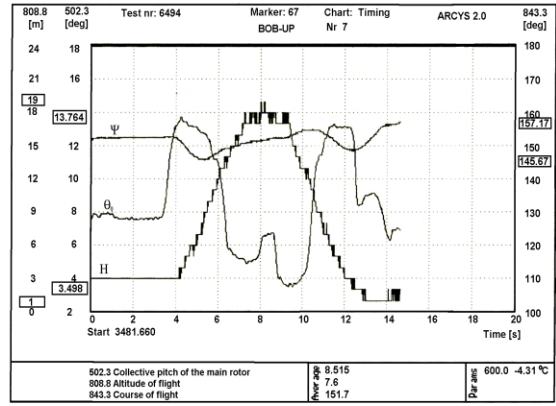


Fig.1 Recorded altitude, collective pitch and course

Comparing courses of parameters obtained from the simulation and from the flight one can observe the good agreement between them. Characters of changes are similar and the extreme values are almost the same. Differences between courses are the result of simplifications of the applied model. The reconstruction of the flight parameters, which were used as the constraints / (3.1)-(3.3) /, is also only approximate.

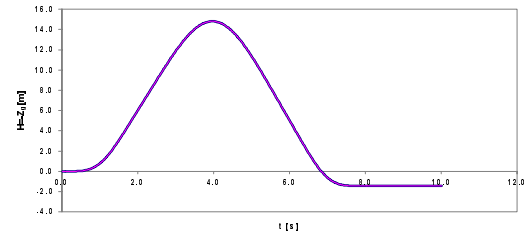


Fig.2 Altitude of flight - simulation

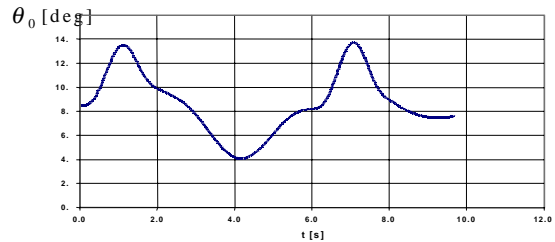


Fig.3 Collective pitch of the main rotor - simulation

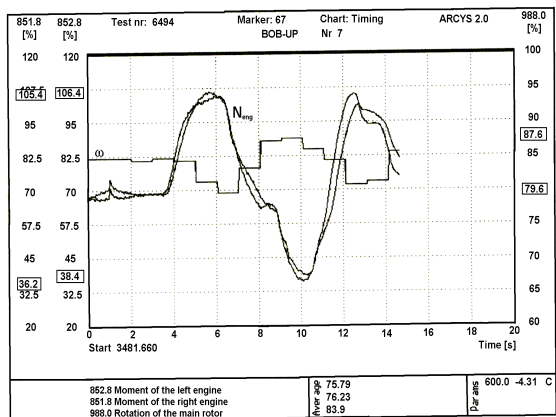


Fig.4 Recorded moments of engines and angular velocity of the main rotor

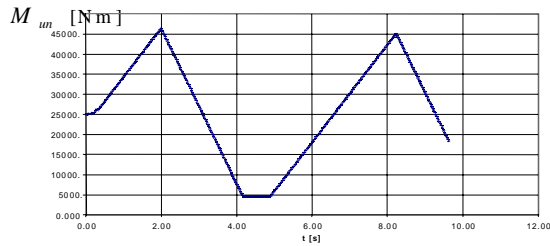


Fig.5 Moment of the power system - simulation

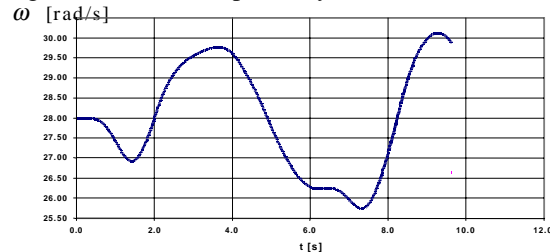


Fig.6 Angular velocity of the main rotor - simulation

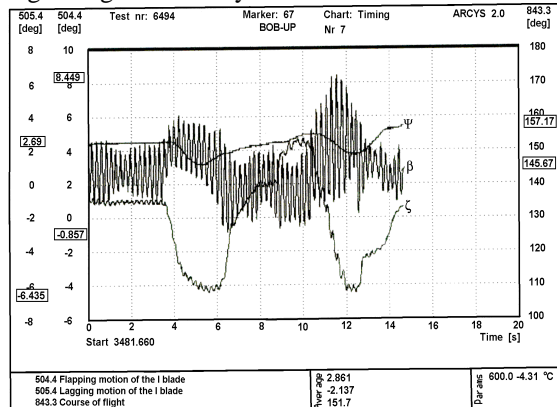


Fig.7 Recorded flapping β , lagging ζ of the blade end course of flight

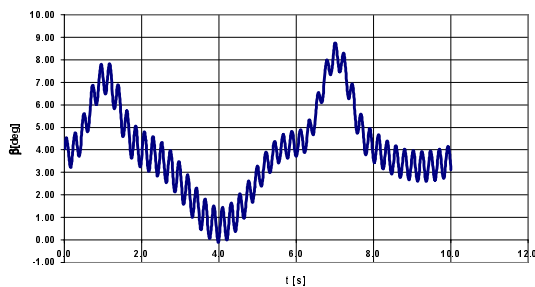


Fig.8 Flapping β - simulation

The bob up and bob down manoeuvre is performed by suitable changes of the collective pitch θ_0 /fig.1, 3/. At the beginning this angle is increased and the helicopter starts climbing /fig.1, 2/. Because the drag moment grows, the angular velocity of the main rotor decreases /fig.4, 6/. The power system reacts by increasing the moment produced by this system /fig.4, 5/. Before the maximum altitude is reached the pilot starts to decrease θ_0 . The minimum of this control angle is obtained when the helicopter reaches the maximum

altitude. When the helicopter is falling the pilot starts to increase θ_0 to brake the falling at a fixed altitude. During this manoeuvre the rotation of the main rotor and the moment of the power system changes. Changes of the average value of the flapping motion /fig.7, 8/ corresponds to changes of the collective pitch θ_0 .

3.2. The failure of the helicopter engine

The failure of the power system is one of the most dangerous cases of a flight. After a decay (total or partial) of the moment produced by the power system many characteristic symptoms occur which are very informative for a pilot. They are as follows:

- Noise of the engines decreases.
- The angular velocity of the main rotor decreases. In only one second it obtains the minimal acceptable value;
- The course of the helicopter changes immediately because of the change of the drag moment forced by the main rotor. /For the Sokol helicopter its fuselage turns right/.
- The helicopter is rolling right because of the left sideslip.
- The pitching angle of the fuselage decreases (nose down) because of a decrease of the thrust of the main rotor. This causes that an angle of attack of the stabiliser is changed.
- The altitude of flight decreases as the result of a drop of the thrust.

Consequences of the failure of the power system depend on the phase of flight, during which the failure appears. The most hazardous is the case when the failure occurs during the hover. The failure appearing during the horizontal flight is less dangerous. Failures appearing during other phases of flight are considered separately. The velocity of a flight has a very important influence on results of the failure.

The most important task after the failure of the power system is a safe landing. Rarely the helicopter can continue its flight with one efficient engine. The emergency landing could be performed in different ways depending on the kind of failure and on the phase of flight. But in all cases the zone, where a landing field may be found, is significantly limited. In the case of the low flight the natural

obstacles may be an additional difficulty. They may confine visibility. Because of it, in some cases the instantaneous increase of flight altitude may be desired – looking for any convenient landing ground may be necessary.

Some numerical simulations of these types of failures were performed. Their results were in agreement with characteristic symptoms described above. On the basis of these simulations the scenario of the real flight was specified. Next, test flights with the engines temporarily turned off were realised. Selected recorded flight and control parameters were used in numerical reconstruction of these flights. Results of one of these simulations are presented below. They are compared with the time courses recorded during flight.

Three angular velocities $P(t)$, $Q(t)$, $R(t)$ and the linear velocity $W(t)$ were applied as the constraints. The spline method was used to define these constraints. Because the velocity $W(t)$ had not been recorded, therefore it was determined on the basis of the time course of the normal overload $N_z(t)$:

$$W(t) = \int_0^t [N_z(\tau) - 1] d\tau \quad (3.3)$$

During the experimental flight the power of engines was rapidly decreased to the minimal value. Pilot observed reactions of the helicopter. He paid the peculiar attention to the angular velocity of the main rotor, rolling and yawing of the helicopter. All flight and control parameters were recorded.

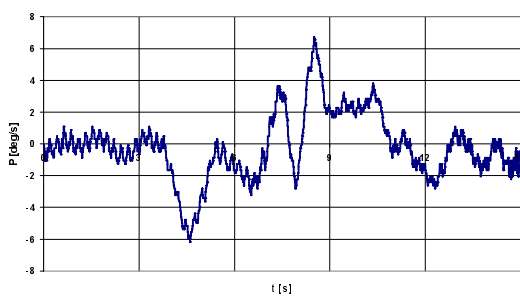


Fig.9 Recorded rolling velocity $P(t)$

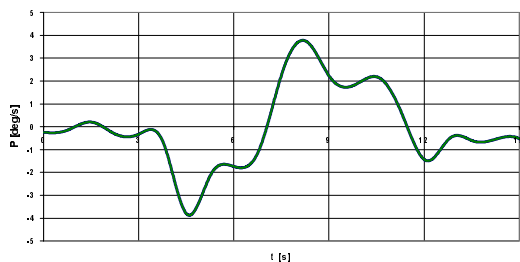


Fig.10 Rolling velocity $P(t)$ - simulation

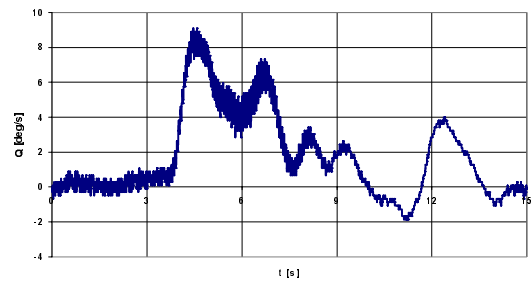


Fig.11 Recorded pitching velocity $Q(t)$

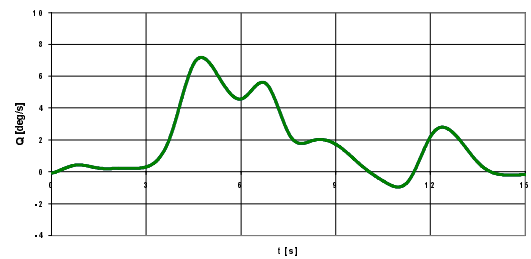


Fig.12 Pitching velocity $Q(t)$ - simulation

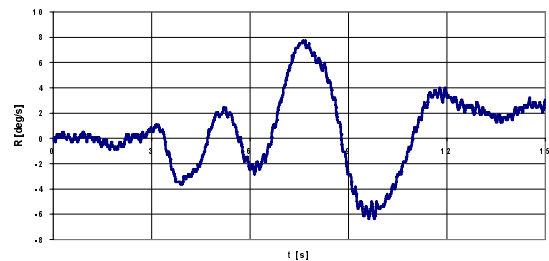


Fig.13 Recorded yawing velocity $R(t)$

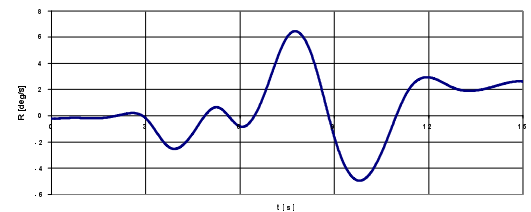


Fig.14 Yawing velocity $R(t)$ - simulation

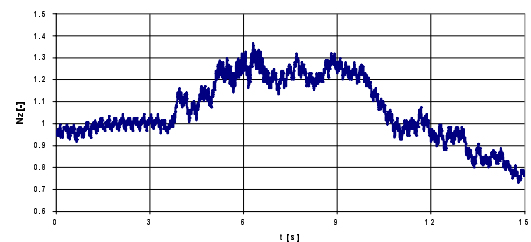


Fig.15 Recorded overload $N_z(t)$

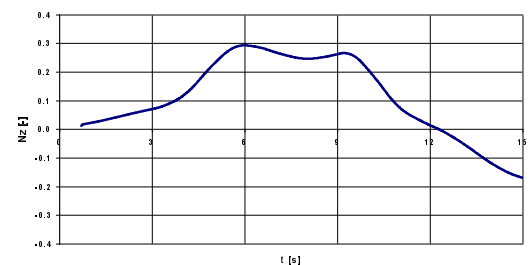


Fig.16 Overload $N_z(t)$ - simulation

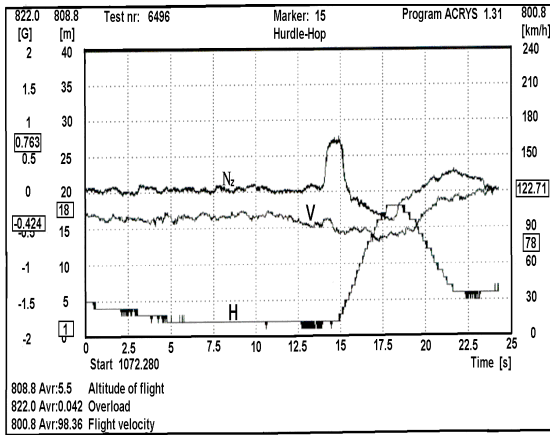


Fig.25 Recorded altitude, flight velocity and normal overload

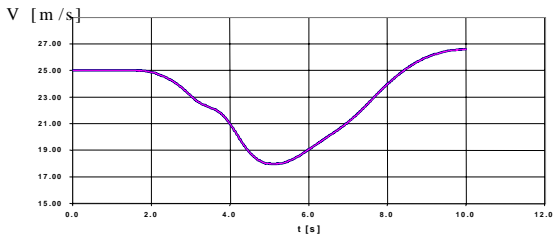


Fig.26 Flight velocity - simulation

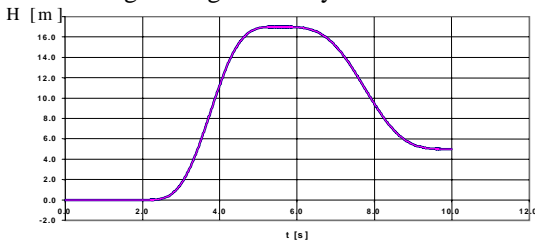


Fig.27 Altitude of flight - simulation

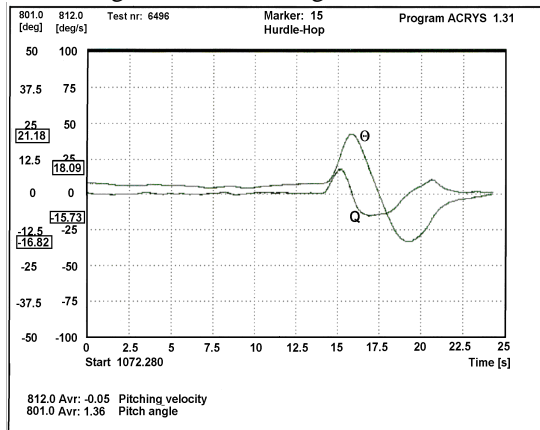


Fig. 28 Recorded pitching velocity and pitch angle

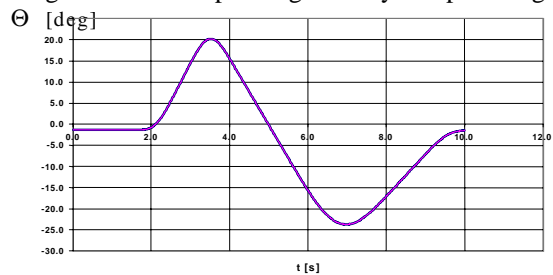


Fig. 29 Pitch angle - simulation

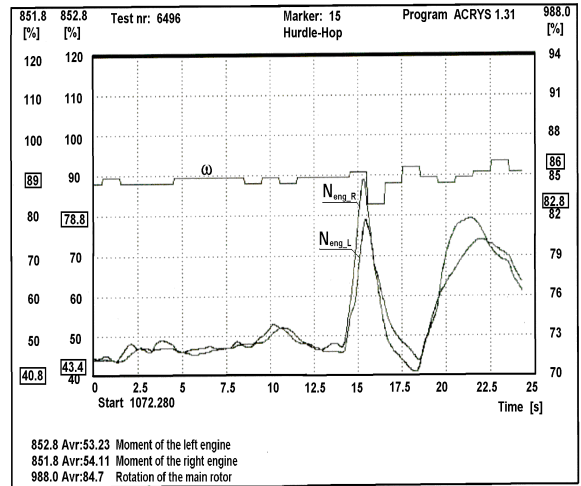


Fig.30 Moments of engines and angular velocity of the main rotor

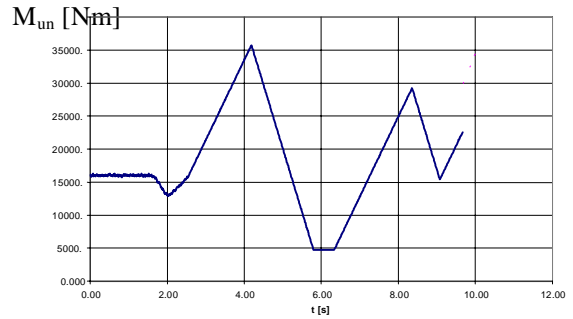


Fig.31 Moments of engines - simulation

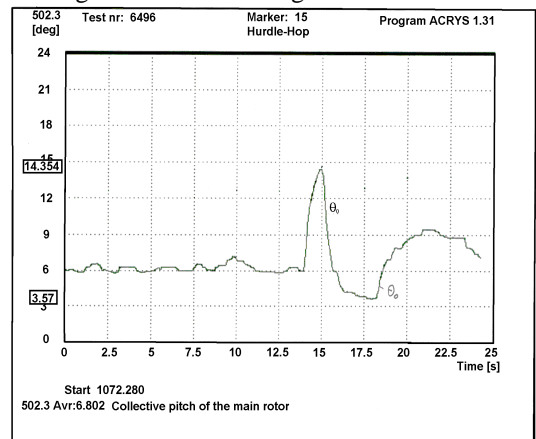


Fig. 32 Recorded collective pitch

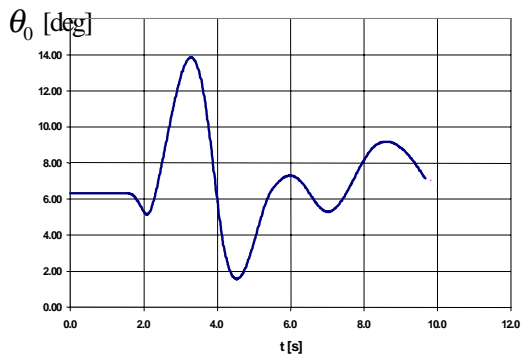


Fig. 33 Collective pitch - simulation

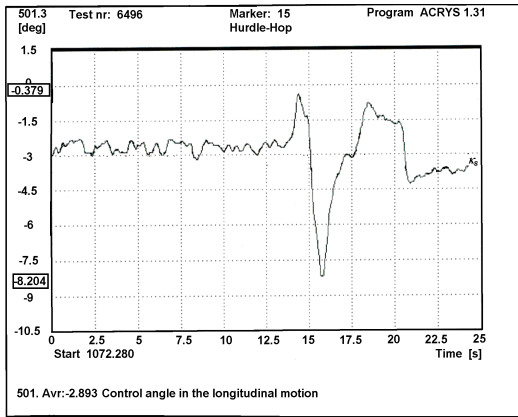


Fig. 34 Recorded control angle in the longitudinal motion

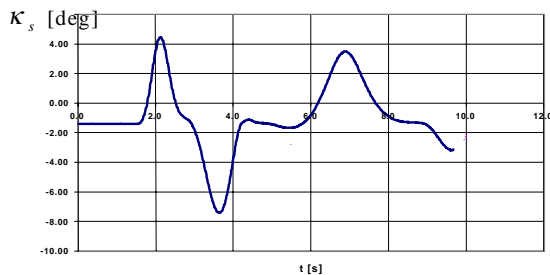


Fig. 35 Control angle in the longitudinal motion - simulation

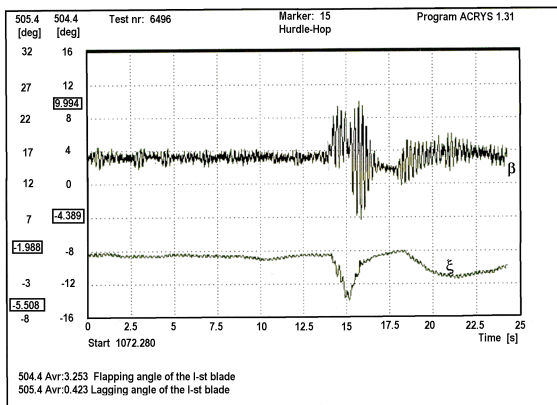


Fig. 36 Recorded flapping angle of the blade

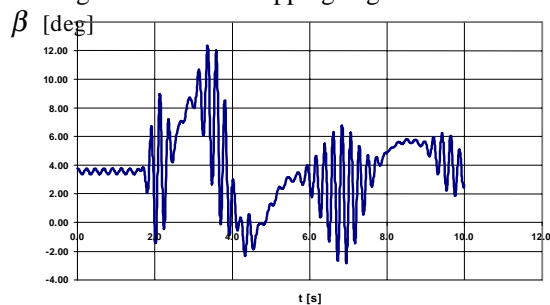


Fig. 37 Flapping angle of the blade - simulation

Conclusions

A relatively simple numerical methodology was applied for determining the controls, which are necessary to perform a constrained flight for

helicopter. On the basis of the performed calculations the following conclusions can be formulated:

1. During numerical calculations a very high accuracy of determining the output vector is required.
2. This accuracy is strictly limited by errors of numerical rounding.
3. High gradients or discontinuities of constraints are causes of the determined controls broadening.
4. The method was not succeeded in determining control signals on the basis of trajectory of flight.

References

1. *Aeronautical Design Standard – Handling Qualities Requirements for Military Rotorcraft*, United States Army Aviation and Troop command, St. Louis, July 1994.
2. Padfield G. D., *Helicopter Flight Dynamics*, Blackwell Science Ltd., Oxford, 1996.
3. Kowaleczko G., *Nonlinear Dynamics of Spatial Motion of a Helicopter*, Military University of Technology, Warsaw, 1998, (in Polish)
4. Kowaleczko G., *Analysis of Dynamics of Spatial Motion of a Helicopter-Autopilot System*, Military University of Technology, Warsaw, 1992, (in Polish)
5. Thomson D. G., Bradley R., „*Development and Validation of an Algorithm for Helicopter Inverse Simulations*”, *Vertica*, vol. 14/2, 1990
6. Hess R., Gao C., Wang S., „*Generalized Technique for Inverse Simulation Applied to Aircraft Flight Control*”, *Journal of Guidance, Control and Dynamics*, vol.14/5, 1991
7. Hess R. A., C. Gao., „*A Generalized Algorithm for Inverse Simulation Applied to Helicopter Maneuvering Flight*”, *Journal of the American Helicopter Society*, vol. 38/4, October 1993
8. Rutherford S., Thomson D., „*Improved Methodology for Inverse Simulation*”, *Aeronautical Journal* vol.100/933, 1996
9. Rutherford S., Thomson D., „*Helicopter Inverse Simulation Incorporating an Individual Blade Rotor Model*”, *Proceedings of 20-th ICAS Congress, Sorrento, 1996*